Magnetic properties of the quasi-two-dimensional antiferromagnet Ni_{0.7}Al_{2}S_{3.7}

Tomoya Higo, Rieko Ishii, Melissa C. Menard, Julia Y. Chan, Hironori Yamaguchi, Masayuki Hagiwara, and Satoru Nakatsuji

Phys. Rev. B **84**, 054422 — Published 8 August 2011

DOI: 10.1103/PhysRevB.84.054422

Magnetic properties of the quasi-two-dimensional antiferromagnet $Ni_{0.7}Al_2S_{3.7}$

Tomoya Higo,[1] Rieko Ishii,[1,*] Melissa C. Menard,[2] Julia Y. Chan,[2]
Hironori Yamaguchi,[3,†] Masayuki Hagiwara,[3] and Satoru Nakatsuji[1,‡]

[1]*Institute for Solid State Physics, University of Tokyo, Kashiwa, Chiba 277-8581, Japan*
[2]*Department of Chemistry, Louisiana State University, Baton Rouge, LA 70803,USA*
[3]*KYOKUGEN, Osaka University, Machikaneyama 1-3, Toyonaka 560-8531, Japan*

(Dated: May 10, 2011)

We report the magnetic properties of the new layered antiferromagnet $Ni_{0.7}Al_2S_{3.7}$. This compound is isostructural to $NiGa_2S_4$, the unique low spin ($S = 1$) two-dimensional (2D) antiferromagnet on the exact triangular lattice. No magnetic long-range order (LRO) was observed in $Ni_{0.7}Al_2S_{3.7}$ down to 0.4 K, as in $NiGa_2S_4$. Instead, a clear spin freezing is observed at $T_f \sim 4$ K, which is one order magnitude smaller than the Weiss temperature $|\theta_W| \sim 55$ K. In contrast with the field independent frustrated magnetism of the pure $NiGa_2S_4$, both the susceptibility and specific heat are found to be strongly field dependent, indicating disorder effects due to vacancies at the Ni and S sites. Under a field of 9 T, however, $Ni_{0.7}Al_2S_{3.7}$ shows a T^2-dependent magnetic specific heat that scales with $|\theta_W|$, similarly to $NiGa_2S_4$. This implies an emergence of a 2D linearly dispersive mode without a magnetic LRO. Electron spin resonance (ESR) measurements reveal a systematic broadening of the resonance spectra on cooling with $T^{-2.5}$, suggesting that Ni spins develop 2D antiferromagnetic correlation with decreasing T toward $T = 0$. Moreover, $Ni_{0.7}Al_2S_{3.7}$ exhibits crossover from a high temperature isotropic to a low temperature easy-plane anisotropic state across $T_A \sim 70$ K. This scale T_A is higher than $|\theta_W|$, and is too large to be attributed either to antiferromagnetic correlation or to single ion anisotropy of Ni^{2+} that is found less than 0.1 K from the ESR experiment. We discuss that ferronematic correlation is a possible origin of the magnetic anisotropy.

PACS numbers: 75.30.Gw, 75.40.Cx, 75.50.Ee

I. INTRODUCTION

Geometrically frustrated magnets have attracted great interest due to the possible emergence of novel spin-disordered states by suppressing conventional magnetic order. In two dimensions (2D), the triangular lattice is one of the simplest forms of a geometrically frustrated lattice with a single magnetic ion in a unit cell, and has been extensively studied to search for spin-disordered states. Although a number of bulk systems with triangular lattice have been studied[1], most have a rather strong interlayer coupling, which leads to a magnetic long-range order.

To date, spin-disordered states have been found only in a few triangular lattice antiferromagnets (AFMs) such as the organic materials κ-(BEDT-TTF)$_2$Cu$_2$(CN)$_3$ ($S = 1/2$)[2], EtMe$_3$Sb[Pd(dmit)$_2$]$_2$ ($S = 1/2$)[3], and inorganic material $NiGa_2S_4$ ($S = 1$)[4,5]. $NiGa_2S_4$ is the first example of a low spin ($S = 1$) AFM on the exact triangular lattice. With a layered structure separated by a van der Waals gap, $NiGa_2S_4$ exhibits essentially 2D magnetism, as revealed by the neutron measurements[4,6].

Despite the large energy scale of the Weiss temperature $\theta_W \sim -80$ K, this material does not form LRO at least down to $T = 0.08$ K[7]. Instead, microscopic resonance experiments have clarified unusual bulk critical slowing down across $T^* = 8.5$ K with a highly extended critical regime down to a characteristic freezing temperature of $T_0 \sim 2$ K[7,8]. In this intermediate temperature regime between T^* and T_0, spins retain slow dynamics with microsecond order time scale, forming a viscous spin liquid[5,9]. Below T_0 where the spins become quasi-static, the temperature dependence of the nuclear relaxation rates and the specific heat have strikingly revealed a linearly dispersive mode in two-dimensions in the absence of magnetic LRO. In the same temperature range, the specific heat shows no field dependence, signaling that the gapless excitations are insensitive to magnetic field[4,5].

Interestingly, spin dependent impurity effects found in the specific heat of $Ni_{1-x}M_xGa_2S_4$ ($M^{2+} = Mn^{2+}$, Fe^{2+}, Co^{2+}, and Zn^{2+}) indicate that the integer size of the Heisenberg spins is essential to stabilize the 2D linearly dispersive mode[10]. This parity dependence suggests quantum magnetism due to biquadratic form of spin exchange interactions, namely, the quadrupolar/spin nematic correlations.

In particular, a study of nonmagnetic impurity effect on $NiGa_2S_4$ found that only 1 % substitution strongly suppresses the coherent behavior. However, the suppression is not perfect and the robust feature of the T^2 dependent specific heat and its scaling behavior with the Weiss temperature is found up to 30 % substitution of Zn for Ni. This clarifies the existence of a coherent Nambu-Goldstone mode[11], whose velocity is one order magnitude slower than the one for 2D antiferromagnetic spin-wave-like excitations revealed by the neutron measurements[6].

Moreover, recent angle resolved photoemission spectroscopy at 100 K has found that low energy hole dynamics is characterized by a different wave vector from the one for a low temperature antiferromagnetic short-range correlation[4,6], indicating that the high temperature state

above T^* is not governed simply by an antiferromagnetic spin excitations[12]. The coherent behavior without LRO and the high temperature unusual critical slowing down toward T^* in $NiGa_2S_4$ has been discussed in terms of spin nematic correlation[13–17], the topological phase transition due to vector spin chirality[18,19], and C_3 bond-order phase transition[17,20]. However, the origin is still open as an important issue.

In order to deepen our understanding of the ground state of $NiGa_2S_4$, we have searched for compounds isostructural to $NiGa_2S_4$ and have succeeded in synthesizing a new material $Ni_{0.7}Al_2S_{3.7}$ ($S = 1$) by displacing Al for Ga ions. Here, we report crystal structure, magnetic and thermal properties of $Ni_{0.7}Al_2S_{3.7}$.

II. EXPERIMENTAL

As starting materials for single crystal growth, polycrystalline samples of $Ni_{0.7}Al_2S_{3.7}$ were synthesized by annealing of Ni, Al, and S with reaction ratio of (1:2:4) in evacuated quartz ampoules for a few days at 900 °C. Single crystals of $Ni_{0.7}Al_2S_{3.7}$ were prepared by chemical vapor transport method in evacuated quartz ampoules. The transport reactions were carried out in a temperature gradient 850-950 °C for a few weeks using iodine as transport agent with a concentration of 3 mg/cm^3.

Synchrotron crystallographic data were collected on single crystals at the Advanced Light Source (ALS) synchrotron facility in Berkley California at the small-crystal crystallography beam-line 11.3.1 (Lawrence Berkley National Laboratory). The data were collected using the program APEX2 and processed using the program SAINT routine within APEX2[21]. The data were corrected for absorption and beam corrections based on the multi-scan technique as implemented in SADABS[22]. Direct methods were used to solve the structures. The model of the structure was refined with SHELX97[23].

Magnetic susceptibility was measured between 2 and 400 K up to 7 T with a commercial SQUID magnetometer, Magnetic Properties Measurement System (MPMS-XL, Quantum Design). Specific heat C_P was measured by a thermal relaxation method between 0.4 and 200 K up to 9 T with a commercial calorimeter, Physical Properties Measurement System (PPMS, Quantum Design).

ESR measurement in pulsed magnetic fields up to about 53 T was carried out at temperatures between 1.3 and about 75 K using pulsed field ESR apparatus equipped with a non-destructive pulse magnet at KYOKUGEN in Osaka University. Submillimeter waves at a frequency from about 500 GHz to about 1.4 THz are generated with a FIR laser and those at the frequency below 500 GHz are obtained by using backward wave oscillator (BWO). ESR signals are detected with an InSb hot-electron bolometer.

III. RESULTS

A. Crystal structure

Crystallographic data are shown in TABLE I. $Ni_{0.7}Al_2S_{3.7}$ crystallizes in trigonal space group P-3m1 (R_1 = 6.16 %) and is isostructural to $NiGa_2S_4$ as shown in Fig.1(a). Lattice parameters of $Ni_{0.7}Al_2S_{3.7}$ at room temperature are a = 3.6060(13) Å and c = 11.98500(12) Å. The large aspect ratio indicates the high two-dimensionality of $Ni_{0.7}Al_2S_{3.7}$. Atomic positional and displacement parameters of $Ni_{0.7}Al_2S_{3.7}$ are listed in TABLE II. This material has a 30 % deficiency at the Ni site of the octahedra. The refined composition is consistent with that determined by SEM-EDX analysis. Thus, given the charge neutrality, Ni ions should be divalent with $t_{2g}^6 e_g^2$ ($S = 1$) configuration. Consistent results were obtained in recent X-ray photoemission spectroscopy measurements, indicating that Ni ions have 2+ valence[24]. Moreover, the effective moment obtained from the analysis of the susceptibility is consistent with the theoretical value for $S = 1$, as mentioned later. As a result, Ni^{2+} ions form a partially filled triangular lattice as illustrated in Fig. 1(b) and (c). Since the lattice parameters of $Ni_{0.7}Al_2S_{3.7}$ are smaller than those of $NiGa_2S_4$, the study on $Ni_{0.7}Al_2S_{3.7}$ may reveal effects of the chemical pressure and/or the site vacancy on the 2D frustrated magnetism of $NiGa_2S_4$.

The edge-sharing octahedra consist of Ni^{2+} are surrounded by six equidistant S^{2-} (2.430(2) Å) and are compressed along the (111) direction with two in-plane angles of 95.81(11)° and 84.19(11)°. The partially occupied, Ni^{2+}-centered octahedra are consistent with the short S^{2-}-S^{2-} contacts in the octahedra (3.2570(5) Å) when compared to $NiGa_2S_4$ (S^{2-}-S^{2-}: 3.625(1) Å). The corner-sharing tetrahedra are comprised of Al^{3+} surrounded by S^{2-} compressed along the c-direction with the apical Al^{3+}-S^{2-} bond (2.2339(4) Å) slightly shorter than the remaining three Al^{3+}-S^{2-} bonds (2.2615(7) Å). When comparing $NiGa_2S_4$ and $Ni_{0.7}Al_2S_{3.7}$, the partial occupancies of Ni^{2+} and S^{2-} coincide with a smaller unit cell than expected upon substitution of Al^{3+} and Ga^{3+} (without occupational disorder) and has been reported for various NiS-containing compounds, including NiS_{1-x}[25,26], Ni_xS_y[27], $Ni_{2.5}MoS_{6.7}$[28], $Ni_{0.45}ZrS_2$[29], $Ni_{0.325}NbS_2$[30], and $Ni_{0.95}Nb_3S_6$[31] phases.

Recent neutron diffraction measurements of $NiGa_2S_4$ have revealed a 2D incommensurate short-range order, which can be attributed to a dominant third nearest neighbor interaction $J_3/k_B \sim 32(7)$ K and weak ferromagnetic nearest neighbor coupling $J_1/k_B \sim 4(1)$ K[6]. This dominant J_3 is also inferred from the photoemission spectroscopy measurement[32]. The "NiS_2" plane of $Ni_{0.7}Al_2S_{3.7}$ has the same structure as that of $NiGa_2S_4$, and should consist of the in-plane superexchange coupling similar to those of $NiGa_2S_4$. Therefore, the dom-

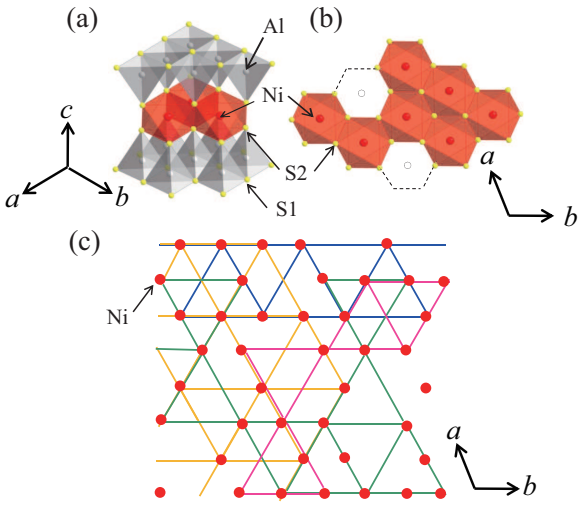

FIG. 1: (color online) (a) Crystal structure of $Ni_{0.7}Al_2S_{3.7}$. (b) NiS_2 layer in $Ni_{0.7}Al_2S_{3.7}$ viewed along the c-axis, which consists of edge-sharing NiS_6 octahedra. Empty Ni sites and the associated NiS_6 octahedra are shown by black circle and by broken line, respectively. (c) Schematic network formed by the third nearest interaction J_3 (pink, blue, green, and yellow lines) on a triangular Ni lattice of $Ni_{0.7}Al_2S_{3.7}$.

space group	P-3m1
a (Å)	3.6060(13)
c (Å)	11.9850(12)
V (Å^3)	134.96(7)
Z	1
$^aR_1$	0.0616

$^aR_1 = \sum(||F_o| - |F_c||)/\sum|F_o|$

TABLE I: Crystallographic data of $Ni_{0.7}Al_2S_{3.7}$ at room temperature.

Atom	Site	x	y	z	Occupancy	$^aU_{eq}$(Å^2)
Ni	1b	0	0	1/2	0.66(3)	0.0136(15)
Al	2d	1/3	2/3	0.2090(4)	1.0	0.0151(16)
S1	2d	1/3	2/3	0.8648(4)	1.0	0.0174(15)
S2	2d	1/3	2/3	0.3955(3)	0.89(3)	0.0104(14)

TABLE II: Refined atomic positional and displacement parameters of $Ni_{0.7}Al_2S_{3.7}$ at room temperature. $^aU_{eq}$ is defined as one third of the trace of the orthogonalized U_{ij} tensor.

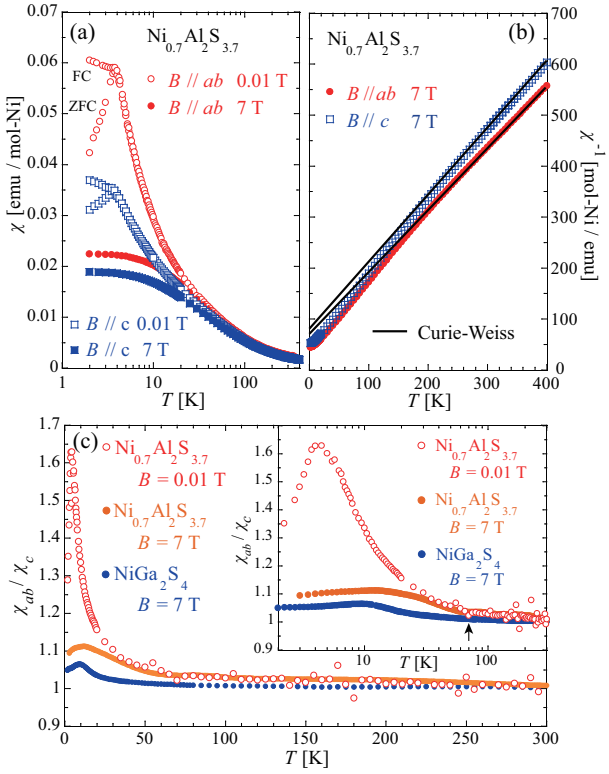

FIG. 2: (color online) (a) Temperature dependence of the susceptibility $\chi \equiv M/B$ of $Ni_{0.7}Al_2S_{3.7}$ under 0.01 T and 7 T for $B \parallel ab$ and $B \parallel c$. There is a hysteresis between FC and ZFC measurement below 4 K at 0.01 T. (b) Temperature dependence of the inverse susceptibility χ^{-1} of $Ni_{0.7}Al_2S_{3.7}$ at 7 T for $B \parallel ab$ (red circle) and $B \parallel c$ (blue square). Solid lines indicate the fit to the Curie-Weiss law. (c) Temperature dependence of the anisotropy ratio χ_{ab}/χ_c obtained for $Ni_{0.7}Al_2S_{3.7}$ under 0.01 T and 7 T and $NiGa_2S_4$ under 7 T[34]. Inset: χ_{ab}/χ_c vs. T in logarithmic scale. A clear enhancement of χ_{ab}/χ_c below 70 K, as indicated by a black arrow, is observed in $Ni_{0.7}Al_2S_{3.7}$.

inant in-plane superexchange coupling in $Ni_{0.7}Al_2S_{3.7}$ should be the third nearest neighbor interaction J_3 and antiferromagnetic. In addition, the nearest neighbor coupling is most likely ferromagnetic as in $NiGa_2S_4$, because the smaller bond angle (95.8°) of the Ni-S-Ni path in $Ni_{0.7}Al_2S_{3.7}$ than that (96.9°) for $NiGa_2S_4$ stabilizes more ferromagnetic coupling. Figure 1(c) presents a schematic configuration of magnetic Ni ions on a NiS_2 layer of $Ni_{0.7}Al_2S_{3.7}$. Ni ions are part of a local triangle made of the third nearest neighbor interaction J_3 (pink, blue, green, and yellow lines), and under the influence of the geometrical frustration. However, the deficiency of the Ni ions causes missing bonds and induces weakly coupled spins. This type of spins is known as "orphan" spins[33], and has relatively low energy magnetic coupling scale and can be easily polarized by application of the field, as we will discuss later. Although the Ni^{2+} spins are diluted by 30 %, the classification of spins into "bulk" and "orphan" spins is useful based on our systematic study of the nonmagnetic impurity effects in $Ni_{1-x}Zn_xGa_2S_4$[11].

B. Susceptibility

The temperature dependence of the susceptibility $\chi(T) \equiv M(T)/B$ at $B = 0.01$ and 7 T is presented in Fig. 2(a). Hysteresis between the field-cooled (FC) and zero-field-cooled (ZFC) data under 0.01 T is seen below a freezing temperature $T_f = 4$ K. This spin glass behavior can be attributed to both the magnetic frustration based on the

triangular lattice symmetry and the randomness due to the deficiency of Ni ions. No sharp magnetic anomaly or hysteresis between the FC and ZFC data was observed down to 2 K under 7 T. The susceptibility data above 200 K follows the Curie-Weiss law, $\chi(T) = C/(T - \theta_{\rm W})$, as shown in Fig. 2(b). Here, C and $\theta_{\rm W}$ are Curie constant and Weiss temperature, respectively. Effective moments are estimated to be $\sim 3.05(7)\mu_{\rm B}$/Ni for $B \parallel ab$ and $\sim 2.92(5)\mu_{\rm B}$/Ni for $B \parallel c$. These are typical values known for Ni^{2+} ions and are slightly larger than the theoretical estimate $2.83\mu_{\rm B}$ for $S = 1$, indicating the contribution from spin-orbit coupling. The Weiss temperatures, $\theta_{\rm W} = -55(1)$ K for $B \parallel ab$ and $-56(1)$ K for $B \parallel c$, indicate the dominant interaction between Ni ions are antiferromagnetic. The ratio $|\theta_{\rm W}|/T_{\rm f} = 14$ is large due to the combination of geometrical frustration, low dimensionality and disorder.

Figure 2(c) shows the ratio of the in-plane susceptibility χ_{ab} and inter-plane susceptibility χ_c as a function of T under 0.01 and 7 T. χ_{ab}/χ_c is enhanced below 70 K, indicating the onset of easy-plane anisotropy at $T < 70$ K. A similar increase in χ_{ab}/χ_c is also seen for $NiGa_2S_4$ below $T \sim 30$ K[34]. Although rapid enhancement of χ_{ab}/χ_c in the low-temperature region of $T < 20$ K under 0.01 T could be attributed to the orphan spins, the appearance of magnetic anisotropy in a high temperature region should be intrinsic to the bulk spins of $Ni_{0.7}Al_2S_{3.7}$.

According to the high temperature expansion analyses on a Heisenberg model with a single ion anisotropy[35], $\mathcal{H} = J\sum_{\langle i,j\rangle} \boldsymbol{S}_i \cdot \boldsymbol{S}_j + D\sum_i (S_i^z)^2 - g\sum_i \boldsymbol{H} \cdot \boldsymbol{S}_i$, the in-plane and out-of-plane susceptibilities, χ_{ab} and χ_c, are given by

$$\chi_{ab} \sim \frac{2}{3}\frac{g^2}{T + 4J - \frac{D}{6}}, \tag{1}$$

$$\chi_c \sim \frac{2}{3}\frac{g^2}{T + 4J + \frac{D}{3}}. \tag{2}$$

Here, g, J, and D are the g-value, the effective superexchange coupling scale, and the single-ion anisotropy constant, respectively. Therefore, the relation between $\theta_{\rm W}$ and D is given by,

$$\theta_{{\rm W}(c)} - \theta_{{\rm W}(ab)} \sim \frac{D}{2}. \tag{3}$$

D is roughly estimated to be 1(1) K, the same order as $D/k_{\rm B} \sim 0.8$ K of $NiGa_2S_4$ estimated by the ESR measurement.[36,37] As we will discuss, the ESR measurement has clarified $D/k_{\rm B} \lesssim 0.1$ K, which is consistent with the above estimate within the error bar.

C. Specific heat

Figure 3(a) indicates the temperature dependence of the specific heat C_P. C_P shows no sharp anomaly down to 0.4 K, indicating absence of LRO for both $B = 0$ and 9 T. In order to estimate the lattice contribution to the specific heat $C_{\rm L}$ of $Ni_{0.7}Al_2S_{3.7}$, we measured C_P of the nonmagnetic, isostructural analogue $ZnIn_2S_4$, and followed the same conversion procedure using the Debye equation as described in Ref. 5. The T dependence of the magnetic specific heat $C_{\rm M}$ was estimated by subtracting $C_{\rm L}$ from C_P (Fig. 3(b)). $C_{\rm M}/T$ has a broad peak at around 5 K for $B = 0$ T, which can be attributed to the evolution of a short-range correlation between Ni spins. Magnetic entropy, $S_{\rm M}$, as shown in Fig. 3(b), has a plateau around 25 K at $\sim 1/4$ of $S_{\rm M} = R\ln 3$, the theoretical total entropy for $S = 1$ spin. This reveals that the low temperature state is highly degenerate, similar to $NiGa_2S_4$[5].

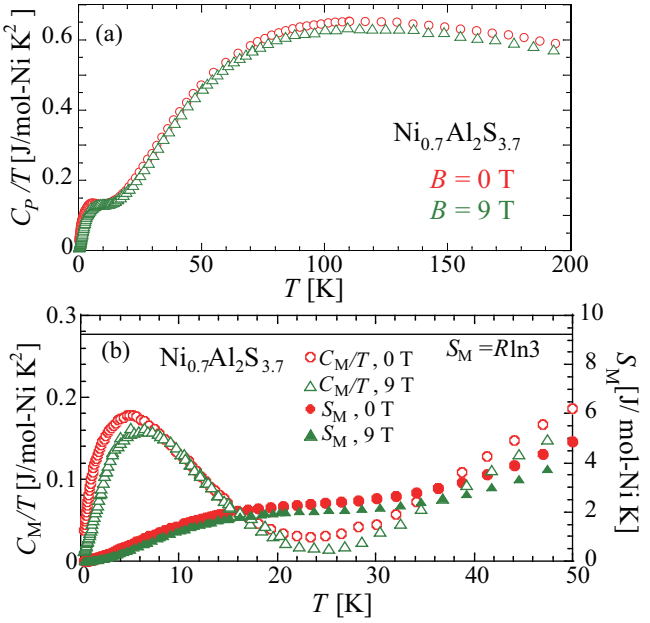

FIG. 3: (color online) Temperature dependence of (a) the total specific heat C_P/T at 0 T (red circle) and 9 T (green triangle), and (b) the magnetic specific heat $C_{\rm M}/T$ (left axis) at 0 T (red open circle) and 9 T (green open triangle), and the magnetic entropy $S_{\rm M}$ at 0 T (red solid circle) and 9 T (green solid triangle) for $B \parallel c$. The horizontal line indicates the theoretical total entropy for $S = 1$, $S_{\rm M} = R\ln 3$.

A prominent behavior at low temperatures in $NiGa_2S_4$ is the T^2-dependence of $C_{\rm M}$ that emerges without magnetic LRO. Similarly in $Ni_{0.7}Al_2S_{3.7}$, $C_{\rm M}$ shows a T^2-dependence below 1 K at 0 T and below 4 K at 9 T (Fig. 4(a)). This behavior is different from a canonical spin glass system that exhibits a T-linear dependence of $C_{\rm M}$ due to local nature of spin fluctuations. Instead, it most likely arises from coherent propagation of a 2D linearly dispersive mode, as observed in $NiGa_2S_4$. The field dependence of $C_{\rm M}$, which is absent in $NiGa_2S_4$, is observed for $Ni_{0.7}Al_2S_{3.7}$ and is possibly due to the orphan spins induced by disorder in $Ni_{0.7}Al_2S_{3.7}$. The orphan spins are much more weakly coupled than the bulk spins and

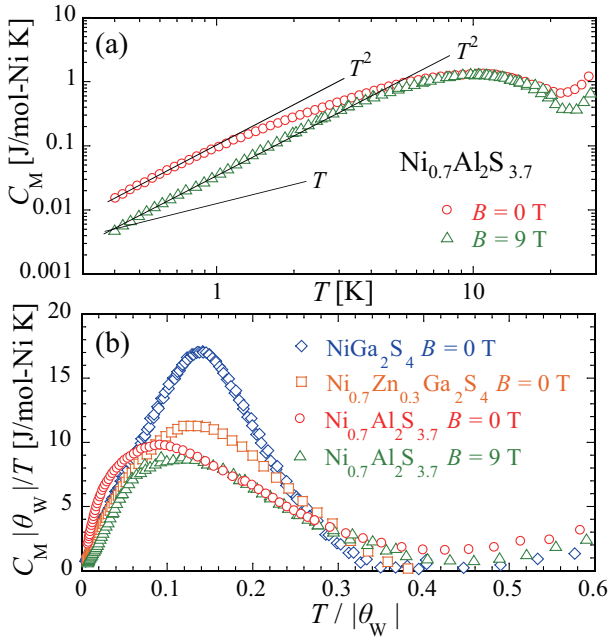

FIG. 4: (color online) (a) Temperature dependence of the magnetic specific heat under 0 T (red circle) and 9 T (green triangle) below 30 K. (b) C_M $|\theta_W|/T$ as a function of $T/|\theta_W|$ in $Ni_{0.7}Al_2S_{3.7}$ at 0 T (red circle) and 9 T (green triangle), $NiGa_2S_4$ at 0 T (purple diamond) and $Ni_{0.7}Zn_{0.3}Ga_2S_4$ at 0 T (orange square) under $B \parallel c$

can be oriented in a relatively small applied field and thus under $\sim$ 9 T. The low temperature specific heat due to the orphan spins may be suppressed due to their Zeeman gap, and the intrinsic T^2 dependence of the specific heat of the bulk spins should become prominent by applying field.

Figure 4(b) provides $C_M|\theta_W|/T$ vs. $T/|\theta_W|$ for $NiGa_2S_4$, $Ni_{0.7}Al_2S_{3.7}$, and $Ni_{0.7}Zn_{0.3}Ga_2S_4$. The T^2-dependent part of the low temperature magnetic specific heat C_M in $NiGa_2S_4$ and $Ni_{0.7}Zn_{0.3}Ga_2S_4$ can be normalized by the single scale of $|\theta_W|$ and its coefficient is proportional to $|\theta_W|^{-2}$.[11,34] This is also the case for $Ni_{0.7}Al_2S_{3.7}$ under 9 T, but the data under 0 T do not exhibit the scaling behavior. This suggests that the data taken at 9 T is intrinsic to the bulk spins since the effects of the orphan spins is suppressed due to the Zeeman gap. The peak of $C_M|\theta_W|/T$ at $T/|\theta_W| \sim 0.14$ is much weaker and broader than that in $NiGa_2S_4$ because of the Ni deficiency in $Ni_{0.7}Al_2S_{3.7}$ as observed in $Ni_{0.7}Zn_{0.3}Ga_2S_4$.

D. Electron spin resonance

Figure 5 shows the temperature dependence of the ESR absorption spectra at 584.8 GHz for $H \| c$. We observed extremely broad resonance signals, which require more than 10 T field range to observe the whole resonance spectra. Thus, we present the spectra at relatively high frequency 584.8 GHz. The resonance field does not shift upon cooling. The g-value along the c-axis is evaluated to be $g_c = 2.07$ from the paramagnetic resonance field well above the Weiss temperature $|\theta_W| \sim 55$ K. The inset of Fig. 5 indicates the temperature dependence of the absorption linewidth (full width at half maximum, FWHM), which increases as the temperature is lowered from the nearly absolute value of the Weiss temperature. In the antiferromagnetic critical region where the antiferromagnetic short-range ordering develops, the temperature dependence of the linewidth is expressed by the following equation,

$$\Delta H_{1/2} \propto (T - T_N)^{-p}, \quad (4)$$

where T_N is the antiferromagnetic long-range ordering temperature and p is a critical exponent which is known to be 2.5 in a 2D Heisenberg AFM.[38] Since no LRO down to 0.4 K was observed, we assume that T_N approximates zero. Then, we fit the experimental linewidths to Eq. (4) with $p = 2.5$ and $T_N = 0$ as shown by the solid line in the inset of Fig. 5. The agreement between them is satisfactory. The difference between experiment and calculation can be attributed to the broadness of linewidth with the large error bars of about ± 5 % of the FWHM values. The frequency dependence of the ESR absorption spectra at 1.3 K for $H \| c$ is demonstrated in Fig. 6(a). The resonance fields are indicated by large arrows. The small signals denoted by small arrows at each frequency arise from an ESR standard sample of DPPH, which is a common abbreviation for an organic chemical compound 2,2-diphenyl-1-picrylhydrazyl, for correction of the magnetic field. The resonance fields are plotted in the frequency-field plane as shown in Fig. 6(b). We compare the resonance mode of this compound with that of $NiGa_2S_4$, which is well fitted to one of the ESR resonance modes calculated based on the 57° spiral spin structure with easy-plane anisotropy.[37] The spin Hamiltonian in this case is written as

$$\mathcal{H} = J_1 \sum_{\langle i,j \rangle} \boldsymbol{S}_i \cdot \boldsymbol{S}_j + J_3 \sum_{\langle l,m \rangle} \boldsymbol{S}_l \cdot \boldsymbol{S}_m + D \sum_i (S_i^z)^2 - g \sum_i \boldsymbol{H} \cdot \boldsymbol{S}_i, \quad (5)$$

where J_1 and J_3 represent the first- and the third-neighbor exchange interactions, respectively, $\langle ij \rangle$ and $\langle lm \rangle$ indicate all the nearest-neighbor and the third-neighbor pairs, respectively, D is an anisotropy constant of the easy-plane type, and the z-axis corresponds to the c-axis. In the case of $NiGa_2S_4$, good agreement between experiment and calculation is obtained with the following parameter values: $J_1/k_B = -4.56$ K, $J_3/k_B = 22.8$ K, and $D/k_B = 0.8$ K, as shown by the dotted line in Fig. 6(b). Since $Ni_{0.7}Al_2S_{3.7}$ is isostructural to $NiGa_2S_4$, we expect the same type of magnetic interactions and anisotropy in both compounds. In addition, considering the 30 % deficiency of Ni at Ni sites in $Ni_{0.7}Al_2S_{3.7}$, the average nearest-neighbor exchange interactions evaluated

from the Weiss temperature $|\theta_W| \sim 55$ K, which is about 70 % of $|\theta_W| \sim 80$ K of $NiGa_2S_4$, must be close to those of $NiGa_2S_4$. Accordingly, we assume that these two compounds have the same exchange interaction constants J_1 and J_3. In that case, the zero-field energy gap of the ESR mode corresponding to the spin-wave excitation energy at $k = 0$, where k is a wave vector, is proportional to $\sqrt{D}$. The observed resonance mode is close to a straight line from zero frequency, which corresponds to $D = 0$, indicated by the broken line in Fig. 6(b). The solid line is drawn as the ESR mode on the assumption of $D/k_B = 0.1$ K, and we thus insist that the magnitude of the anisotropy constant D/k_B is less than 0.1 K. However, it is hard to evaluate the D value precisely due to the lack of the resonance field data at low frequencies below about 300 GHz.

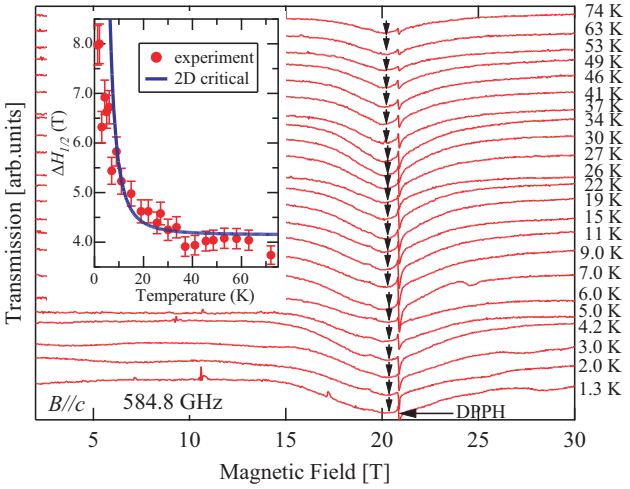

FIG. 5: (Color online) Temperature dependence of the ESR absorption spectra of $Ni_{0.7}Al_2S_{3.7}$ at 584.8 GHz for $H \| c$. The arrows indicate the resonance fields. The sharp small signals come from the ESR standard sample of DPPH for correction of the magnetic field. The inset shows the temperature dependence of the full width at half maximum (FWHM) of the ESR spectra. The error bars with about 5 % of the FWHM values are put on the data. The solid line represents the result of a fit of the experimental data to Eq. (4).

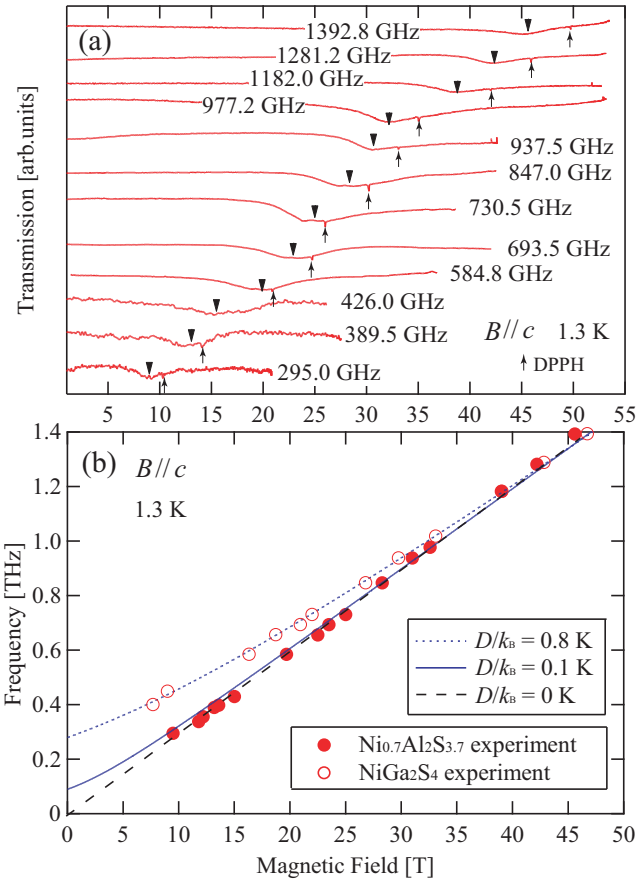

FIG. 6: (Color online) (a) Frequency dependence of the ESR absorption spectra of $Ni_{0.7}Al_2S_{3.7}$ at 1.3 K for $H \| c$. The large and small arrows indicate the resonance fields of $Ni_{0.7}Al_2S_{3.7}$ and the ESR standard DPPH, respectively. (b) Frequency-field plot of the resonance fields at 1.3 K for $H \| c$. The open and closed circles denote the resonance fields of $NiGa_2S_4$ and $Ni_{0.7}Al_2S_{3.7}$, respectively. The dotted, solid, and broken lines represent calculated ESR modes with different values of easy-plane anisotropy $D/k_B = 0.8$ K, 0.1 K, and 0 K, respectively.

IV. DISCUSSION

Let us discuss the origin of the easy-plane anisotropy seen below 70 K. When a magnet has single ion anisotropy, D, the anisotropy should appear below a characteristic temperature scale,

$$T_A \sim D \cdot \left(\frac{\xi}{a}\right)^2. \quad (6)$$

Here, a and ξ are the distance between the nearest neighbor magnetic ions and the magnetic correlation length at T_A, respectively. Given $T_A \sim 70$ K and $D/k_B \lesssim 0.1$ K of $Ni_{0.7}Al_2S_{3.7}$, the correlation length of an antiferromagnetic short-range order should be of the order of $10a$. This is unexpectedly large at this high temperature and comparable to $\xi \sim 7a$ at 1.5 K for $NiGa_2S_4$ obtained by the neutron diffraction measurement[6]. In order to form a short-range order with such a long correlation length at 70 K, the dominant exchange interaction J_3 must be much larger than $J_3/k_B \sim 30$ K of $NiGa_2S_4$. However, the Weiss temperature of $Ni_{0.7}Al_2S_{3.7}$, $|\theta_W| \sim 55$ K, is actually smaller than $|\theta_W| \sim 80$ K of $NiGa_2S_4$, and thus this scenario is highly unlikely.

Another possible origin of the easy-plane anisotropy is a ferronematic ordering[14–16], that is, a spontaneous uniform order of a magnetic quadrupole at each site without freezing of spin dipoles. In the purely Heisenberg spin case, the magnetic anisotropy appears at the fer-

ronematic transition as the direct consequence of spontaneous spatial symmetry breaking of spin fluctuations. However, in the presence of the easy-plane anisotropy as in the present case, only a crossover may occur as a function of temperature. Thus, the easy-plane magnetic anisotropy could be understood due to the crossover in the anisotropy of the spin fluctuations that have the preferential axis within the plane below $T \sim T_{\rm A}$ (= 70 K), otherwise being isotropic at high temperatures. This type of ferronematic state has been discussed in the context of several theories developed to explain the low temperature spin-disordered state of $NiGa_2S_4$[14–17]. Among them, the model proposed by E. M. Stoudenmire *et al.*[17] is the most realistic because it is the only theory that accounts not only for the biquadratic coupling, but for both the ferromagnetic J_1 and antiferromagnetic J_3 interactions.

$Ni_{0.7}Al_2S_{3.7}$ possesses the following properties that meet the conditions for the theoretical model discussed by E. M. Stoudenmire *et al.*[17]. First, the high two-dimensionality of $Ni_{0.7}Al_2S_{3.7}$ is due to the van der Waals gap which significantly weakens the interlayer couplings, the same as in $NiGa_2S_4$. Consequently, no magnetic and/or quadrupolar transitions are observed down to 0.4 K[4–6]. Secondly, spins must be of the Heisenberg type isotropy. Due to the closed-shell configuration of the Ni^{2+} ions, the single-ion anisotropy of $Ni_{0.7}Al_2S_{3.7}$ is indeed small with $D/k_{\rm B} \lesssim 0.1$ K. The third criterion is the structure of the NiS_2 plane that is made of the edge-sharing NiS_6 octahedra. The angle $\sim 100^\circ$ of the Ni-S-Ni bond suppresses the nearest neighbor coupling J_1 and makes the third nearest neighbor coupling J_3 dominant, as found in $NiGa_2S_4$. This weak nearest neighbor coupling would instead allow the biquadratic coupling K to be relatively large. Indeed, K may be enhanced in this particular structure, which has nearly rectangular Ni-S-Ni bond, leading to the weak ferromagnetic nearest neighbor coupling. This nearest neighbor coupling is very sensitive to the bond angle, and thus virtual fluctuations of the lattice that change the bond angle may affect the effective spin Hamiltonian by enhancing the ferro-type biquadratic coupling K, and may stabilize the ferronematic state.

Finally, the T^2-dependent specific heat as well as the spin freezing behavior found in the susceptibility at low temperatures might be associated with the C_3 bond-order phase transition, as has been discussed in E. M. Stoudenmire *et al.*[17]. However, other scenarios including Z_2 vortex biding transition[18,19] are still possible, and the origin is open for the future investigation.

V. CONCLUSION

We synthesized and investigated the magnetic properties of $Ni_{0.7}Al_2S_{3.7}$, the new 2D triangular lattice antiferromagnet with easy-plane anisotropy. While $Ni_{0.7}Al_2S_{3.7}$ has 30 % deficiency of the Ni ion, this compound exhibits a spin-disordered ground state with a clear spin freezing at $T_{\rm f} \sim 4$ K, one order magnitude smaller temperature than the Weiss temperature $\theta_{\rm W} \sim -55$ K. Several interesting phenomena feature the magnetism of $Ni_{0.7}Al_2S_{3.7}$. One is the T^2-dependence of the magnetic specific heat and its scaling behavior with $|\theta_{\rm W}|$, suggesting the emergence of a 2D Nambu-Goldstone mode without a magnetic LRO, as seen in $NiGa_2S_4$. Secondly, ESR measurements show a systematic broadening of the resonance spectra on cooling, suggesting 2D antiferromagnetism with critical slowing down as $T \to 0$. Finally, $Ni_{0.7}Al_2S_{3.7}$ exhibits an easy-plane anisotropy that emerges below 70 K despite its small single ion anisotropy scale $D/k_{\rm B} \lesssim 0.1$ K found by the ESR measurements. While the effect of orphan spins due to the deficiency of Ni should be carefully considered, one likely origin to understand the anisotropy is the ferronematic correlation.

ACKNOWLEDGMENT

We thank T. Momoi, T. Koretsune, T. Mizokawa, Y. Wakisaka, E. Nishibori, H. Sawa, Y. Kiuchi, M. Ichihara, C. Broholm, Y. Nambu, K. Ohgushi, and Y. Maeno for collaboration and enlightening discussions. This work is partially supported by Grant-in-Aid (No. 20340089, No.21684019) from the Japanese Society for the Promotion of Science, and also Grant-in Aid for Scientific Research on Priority Area (No.19052003, No.1702005), and by Global COE Program from the Ministry of Education, Culture, Sports, Science and Technology, Japan. ALS is supported by the U.S. Department of Energy, Office of Energy Sciences Materials Sciences Division, under contract DE-AC02-05CH11231. J.Y.C. and M.M. acknowledge NSF-DMR0756281 for partial support of this project.

* Present address: KYOKUGEN, Osaka University, Machikaneyama 1-3, Toyonaka 560-8531, Japan
† Present address: Department of Physical Science, Osaka Prefecture University, 1-1 Gakuen-cho, Naka-ku, Sakai, Osaka 599-8531, Japan
‡ Electronic address: satoru@issp.u-tokyo.ac.jp

[1] M. F. Collins and O. A. Petrenko, Can. J. Phys. **75**, 605 (1997).
[2] Y. Shimizu, K. Miyagawa, K. Kanoda, M. Maesato, and G. Saito, Phys. Rev. Lett. **91**, 107001 (2003).
[3] T. Itou, A. Oyamada, S. Maegawa, M. Tamura, and R. Kato, Phys. Rev. B **77**, 104413 (2008).
[4] S. Nakatsuji, Y. Nambu, H. Tonomura, O. Sakai, S. Jonas, C. Broholm, H. Tsunetsugu, Y. Qiu, and Y. Maeno, Science **309**, 1697 (2005).
[5] S. Nakatsuji, Y.Nambu, and S. Onoda, J. Phys. Soc. Jpn. **79**, 011003 (2010).
[6] C. Stock, S. Jonas, C. Broholm, S. Nakatsuji, Y. Nambu, K. Onuma, Y. Maeno, and J.-H. Chung, Phys. Rev. Lett. **105**, 037402 (2010).
[7] H. Takeya, K. Ishida, K. Kitagawa, Y. Ihara, K. Onuma, Y. Maeno, Y. Nambu, S. Nakatsuji, D. E. MacLaughlin, A. Koda, and R. Kadono, Phys. Rev B **77**, 054429 (2008).
[8] D. E. MacLaughlin, Y. Nambu, S. Nakatsuji, R. H. Heffner, L. Shu, O. O. Bernal, and K. Ishida, Phys. Rev B **78**, 220403(R) (2008).
[9] Y. Nambu and S. Nakatsuji, in preparation.
[10] Y. Nambu, S. Nakatsuji, Y. Maeno, E. K. Okudzeto, and J. Y. Chan, Phys. Rev. Lett. **101**, 207204 (2008).
[11] Y. Nambu, S. Nakatsuji, and Y. Maeno, J. Phys. Soc. Jpn. **75**, 043711 (2006).
[12] K. Takubo, Y. Nambu, S. Nakatsuji, Y. Wakisaka, T. Sudayama, D. Fournier, G. Levy, A. Damascelli, M. Arita, H. Namatame, M. Taniguchi, and T. Mizokawa, Phys. Rev. Lett. **104**, 226404 (2010).
[13] H. Tsunetsugu and M. Arikawa, J. Phys. Soc. Jpn. **75**, 083701 (2006).
[14] P. Li, G. M. Zhang and S. Q. Shen, Phys. Rev. B **75**, 104420 (2007).
[15] A. Läuchli, F. Mila, and K. Penc, Phys. Rev. Lett. **97**, 087205 (2006).
[16] S. Bhattacharjee, V. B. Shenoy, and T. Senthil, Phys. Rev. B **74**, 092406 (2006).
[17] E. M. Stoudenmire, S. Trebst, and L. Balents, Phys. Rev. B **79**, 214436 (2009).
[18] H. Kawamura and A. Yamamoto, J. Phys. Soc. Jpn. **76**, 073704 (2007).
[19] H. Kawamura, A. Yamamoto, and T. Okubo, J. Phys. Soc. Jpn. **79**, 023701 (2010).
[20] R. Tamura and N. Kawashima, J. Phys. Soc. Jpn. **77**, 103002 (2008).
[21] Bruker *SAINT Version 7.6A Software Reference Manual*, Bruker AXS Inc.: Madison, Wisconsin, USA, 2007.
[22] G. M. Sheldrick, *SADABS v2008/1 semi-empirical absorption and beam correction program*, University of Göttingen, Germany, 2008.
[23] G. M. Sheldrick, Acta Crystallogr. A **64**, 112 (2008).
[24] Y. Wakisaka and T. Mizokawa, (unpublished).
[25] E. Nowack, D. Schwarzenbach, W. Gonschorek, and T. Hahn, Z. Kristallogr. **186**, 213 (1989).
[26] E. Nowack, D. Schwarzenbach, and T. Hahn, Acta Cryst. B**47**, 650 (1991).
[27] M. E. Fleet, Acta Cryst. B**28**, 1237 (1972).
[28] C. L. Chang, Y. K. Tao, J. S. Swinnea, and H. Steinfink, Acta Cryst. C**43**, 1461 (1987).
[29] L. Trichet, J. Rouxel, and J. Cousseau, C. R. Acad. Sci. C Chim. **274**, 394 (1972).
[30] B. Van Laar, H. M. Rietveld, and D. J. W. Ijdo, J. Solid State Chem. **3**, 154 (1971).
[31] K. Anzenhofer, J. M. Van Den Berg, P. Cossee, and J. N. Helle, J. Phys. Chem. Solids **31**, 1057 (1970).
[32] K. Takubo, T. Mizokawa, J.-Y. Son, Y. Nambu, S. Nakatsuji, and Y. Maeno, Phys. Rev. Lett. **99**, 037203 (2007).
[33] P. Schiffer and I. Daruka: Phys. Rev. B **56**, 13712 (1997).
[34] S. Nakatsuji, H. Tonomura, K. Onuma, Y. Nambu, O. Sakai, Y. Maeno, R. T. Macaluso, and J. Y. Chan, Phys. Rev. Lett. **99**, 157203 (2007).
[35] T. Koretsune and T. Momoi, (unpublished).
[36] H. Yamaguchi, S. Kimura, M. Hagiwara, Y. Nambu, S. Nakatsuji, Y. Maeno, and K. Kindo, Phys. Rev B **78**, 180404 (2008).
[37] H. Yamaguchi, S. Kimura, M. Hagiwara, Y. Nambu, S. Nakatsuji, Y. Maeno, A. Matsuo, and K. Kindo, J. Phys. Soc. Jpn. **79**, 054710 (2010).
[38] H. Benner and J. P. Boucher: *Magnetic Properties of Layered Transition Metal Compounds*, ed. L. J. de Jongh (Kluwer Academic Publishers, Dordrecht, 1990), p. 323.